Colossal Effects in Transition Metal Oxides Caused by Intrinsic Inhomogeneities

J. Burgy,[1] M. Mayr,[1] V. Martin-Mayor,[2] A. Moreo,[1] and E. Dagotto[1]

[1]*National High Magnetic Field Lab, Florida State University, Tallahassee, Florida 32306*

[2]*Dipartimento di Fisica, Università di Roma "La Sapienza," Piazzale Aldo Moro 2, 00185 Roma, Italy*

(Received 20 June 2001; published 13 December 2001)

The influence of quenched disorder on the competition between ordered states separated by a first-order transition is investigated. A phase diagram with features resembling quantum-critical behavior is observed, even using classical models. The low-temperature paramagnetic regime consists of coexisting ordered clusters, with randomly oriented order parameters. Extended to manganites, this state is argued to have a colossal magnetoresistance effect. A scale T^* for cluster formation is discussed. This is the analog of the Griffiths temperature, but for the case of two competing orders, producing a strong susceptibility to external fields. Cuprates may have similar features, compatible with the large proximity effect of the very underdoped regime.

DOI: 10.1103/PhysRevLett.87.277202 PACS numbers: 75.10.–b, 71.10.–w, 75.30.Kz

Complex phenomena such as "colossal" magnetoresistance (CMR) in manganites and high-temperature superconductivity (HTS) in cuprates have challenged our understanding of correlated electrons [1]. Recent developments unveiled a previously mostly ignored aspect of doped transition metal oxides (TMO): these systems are *intrinsically inhomogeneous*, even in the best crystals. (i) The evidence in the CMR context is overwhelming. Experiments and theory provide a picture where competing ferromagnetic (FM) and charge-ordered (CO) states form microscopic and/or mesoscopic coexisting clusters [2,3]. Exciting recent experiments [4] identified features referred to as a "quantum-critical point" (QCP) [5]—defined as the drastic reduction of ordering temperatures near the zero-temperature ($T = 0$) transition between ordered states—by modifying the A-site cation mean radius $\langle r_A \rangle$ by chemical substitution at fixed hole density (left inset of Fig. 1). The paramagnetic state in the QCP region—where the Curie temperature T_C is the lowest—is crucial to understand CMR phenomenology, producing the largest CMR ratio [1–3]. (ii) In the HTS context, scanning tunneling microscopy studies of superconducting (SC) Bi2212 revealed a complex surface with nm-size coexisting clusters [8]. Underdoped cuprates also appear to be inhomogeneous [9]. In addition, a colossal proximity effect (CPE) was reported on underdoped $YBa_2Cu_3O_{6+x}$ over large distances [10].

In this paper, the competition between two ordered states in the presence of quenched disorder is investigated. These states are assumed sufficiently "different" that their low-T transition in the clean limit has *first-order* characteristics. The approach has similarities with the classical work of Imry and Ma [11]. From the general considerations, doped TMOs are here considered, with intrinsic disorder caused by chemical substitution. For Mn oxides, a possible rationalization of the CMR effect is discussed, with predictions including a scale T^* for cluster formation—the analog of the Griffiths temperature [12] but in the regime of competing orders. For underdoped Cu oxides, a similar inhomogeneous picture is proposed. The calculations are mainly carried out using a two-dimensional (2D) toy model of Ising spins, but similar data in three dimensions (3D) and for the one-orbital manganite model have also been gathered. Then, our conclusions appear valid for a variety of models with competing orders. The actual Hamiltonian employed here, defined on a square/cubic lattice (spacing $a = 1$) and with Ising variables, is $H = J_1 \sum_{\langle \mathbf{ij} \rangle} S^z_{\mathbf{i}} S^z_{\mathbf{j}} + J_2 \sum_{\langle \mathbf{im} \rangle} S^z_{\mathbf{i}} S^z_{\mathbf{m}} + J_4 \sum_{\langle \mathbf{in} \rangle} S^z_{\mathbf{i}} S^z_{\mathbf{n}}$, in a standard notation. Sites $\langle \mathbf{ij} \rangle$ are at distance 1 (usual nearest neighbors), $\langle \mathbf{im} \rangle$ are at distance $\sqrt{2}$, and $\langle \mathbf{in} \rangle$ are at distance $\sqrt{5}$. The three couplings are antiferromagnetic (AF). More than one coupling is needed to generate two competing $T = 0$ states, and J_1 and J_2 are the natural ones. However, the clean-limit first-order transition between those states was found to be more robust if a small $J_4 \sim 0.2 J_1$ coupling is added. The resulting competing states O_1 and O_2 are an AF state for low J_2/J_1, and a "collinear" AF state with rows (or columns) of spins up and down for large J_2/J_1 [13]. The main features of the toy model phase diagram are common to a variety of models with competing tendencies.

The toy model phase diagram, without disorder, is shown in Fig. 1, and it has the expected shape: the ordering temperatures decrease and meet at the clean-limit critical coupling $J_{2c} = 0.7 J_1$, and the low-T transition was found to be clearly first order. The most interesting result in Fig. 1 is the influence of disorder on the clean-limit diagram. The first-order transitions become continuous with sufficiently large disorder, in agreement with previous work [14]. Critical temperatures far from J_{2c} are not affected much by the disorder strengths considered. However, a *drastic* reduction is observed near J_{2c}. In fact, the Monte Carlo (MC) results suggest that the obtained phase diagram is similar to the insets of Fig. 1 for Mn and Cu oxides. With increasing disorder strength W, either a first-order line separating the competing phases still survives at J_{2c} (red points), as in manganites, or a disordered region of finite J_2 width opens at $T = 0$ (blue points), as in single-layer cuprates. Note that the

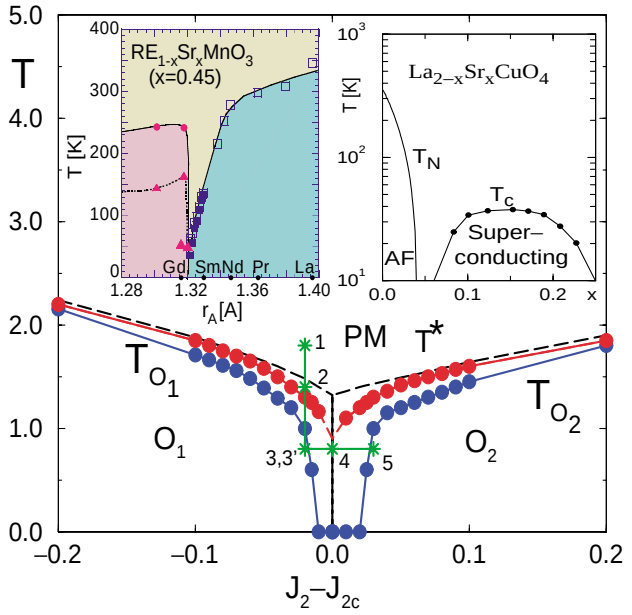

FIG. 1 (color). Phase diagram of the 2D J_1-J_2-J_4 toy model used to analyze the competition between ordered states. Results on 32^3 lattices (not shown) lead to a qualitatively similar phase diagram. $J_1 = 1$ is the scale, and J_4 is fixed to 0.2. Disorder is incorporated such that $J_2(\mathbf{ij})$ at a link joining sites $\mathbf{i}$ and $\mathbf{j}$ is uniformly distributed between $J_2 - W/2$ and $J_2 + W/2$. The blue (red) curve corresponds to $W = 1.5$ ($W = 0.75$). The dashed black lines are the result without disorder $W = 0$, and T^* denotes the clean-limit transition. A Metropolis algorithm was used, on up to 512^2 lattices, calculating (i) the largest ordered cluster size [6] and (ii) the order parameters for AF and collinear phases with a spin structure factor maximized at momenta (π, π) and $(\pi, 0) - (0, \pi)$, respectively. Ten or more realizations of disorder were used, found to be sufficient for large systems. The insets are the phase diagrams of Mn oxides in the FM-CO competition region [4], and of the single-layer Cu oxide in standard notation [7]. Points 1–5 are explained in Fig. 2.

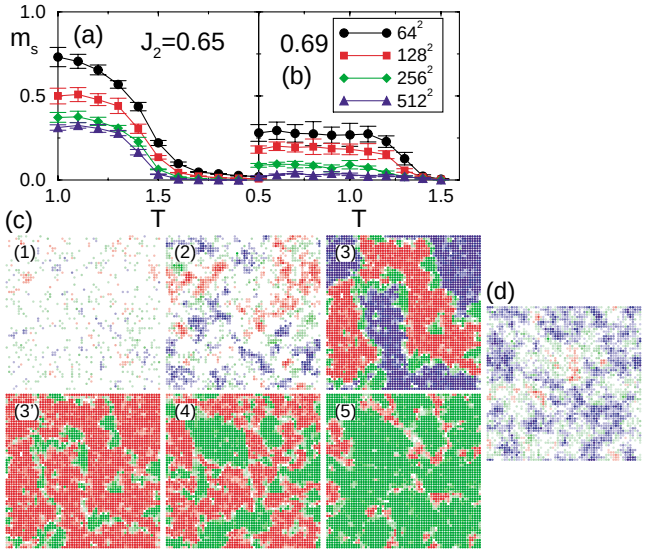

FIG. 2 (color). AF order parameter vs T for the toy model at fixed $W = 1.5$, using several lattice sizes with periodic boundary conditions. (a) corresponds to $J_2 = 0.65$ and (b) corresponds to $J_2 = 0.69$. Note in the latter the order-parameter rapid suppression as the size grows. (c) Typical spin configurations representative of dominant 2D states. Shown are averages over ten measurements, in about 100 MC sweeps to avoid correlations, after thermalizing with thousands of sweeps. Very similar results were obtained in 3D simulations. [(1), (2), (3)] are at $J_2 = 0.68$, and $T = 2.00$, 1.45 (near the resistance peak; see Fig. 3), and 0.80, respectively (see Fig. 1). The green regions have collinear order, while red and blue indicate Néel and "anti-Néel" order, respectively. The last two differ in the staggered order parameter sign, i.e., they intuitively are ↑↓↑↓ ... and ↓↑↓↑ .... The white does not have a dominant order after the MC sweeps considered here. Green/red/blue pale regions have weak order. (3′,4,5) corresponds to $T = 0.8$ and $J_2 = 0.68$, 0.70, and 0.73, respectively (see Fig. 1), and the Néel and anti-Néel states are here given the same color (red), while green remains collinear. (d) Typical spin configuration at staggered field $H_s = 0.01$, $J_2 = 0.68$, $W = 1.5$, and $T = 1.45$.

ordering temperatures exactly meet at $T = 0$ for only one fine-tuned W. However, the overall shape of the phase diagram resembles QCP behavior in a robust range of W. For this reason, our results are qualitatively described as inducing "quantum-critical-point–like" behavior, not a rigorous expression but hopefully descriptive enough to be useful.

Sufficiently strong quenched disorder will smooth first-order transitions [14]. At J_{2c}, this should occur at infinitesimal W in 2D [11], while a finite W is needed in 3D. Then, at J_{2c} and with finite temperature, a paramagnetic state must be generated with growing disorder. Note also that our toy model is classical, but QCP-like behavior is nevertheless generated [15].

Figure 1 is the result of a systematic computational effort. As an example, in Figs. 2a and 2b, the AF order parameter vs T is shown for J_2 values outside and inside the coupling range where a $T = 0$ disordered regime is obtained. For $J_2 = 0.69$ note the order-parameter cancellation with increasing size (this coupling is not critical at $T \neq 0$). Representative spin configurations are in Fig. 2c. Keeping J_2 constant and varying T, three regimes are observed: (1) A high-T regime, where the system is disordered after MC time averaging; (2) an intermediate region $T_{O_1} < T < T^*$ with preformed clusters, but with uncorrelated order parameters giving a globally *paramagnetic* state, similar to the Griffiths phase; (3) a low-T regime where the clusters from (2) grow in size, although the disorder is *uncorrelated* from link to link, and percolate upon cooling. Note that clusters with different signs for the order parameter are separated by thin regions of the competing phase, providing a possible mechanism for stabilizing domain walls. Considering now fixed low-T but changing J_2, configurations [(3′), (4), (5)] are obtained. In this case, just the two ordered phases are in competition (no white regions), and the transition between phases appears percolativelike.

The main features of the results in Figs. 1 and 2—shape, clustered structure, the QCP-like behavior—are believed

to be qualitatively general. In fact, simulations of one-orbital models (below) and other models studied in this effort give a similar phase diagram. Of course, the analogy should not be taken too far, e.g., critical exponents may not be universal since the Ising model underlying symmetries are quite different from those of realistic systems. However, it is worth investigating the consequences of the general phase diagram Fig. 1 for materials where two states strongly compete, such as in Mn oxides. In this context, if a simulation of a realistic model with FM and AF phases on a huge lattice were possible, FM and AF clusters analogous to Fig. 2 would be found. Then, a reasonable way to bypass that (currently impossible) computational effort is to simply translate Fig. 2 into manganite language. This is speculation, but hopefully the essence of the problem is preserved by the procedure. The proposed translation links order O_1 with ferromagnetism, with order parameters pointing in different directions for different clusters, while O_2 corresponds to charge ordering. Translating Fig. 2c(2) into Mn-oxide language leads schematically to Fig. 3a, our proposed CMR state. The preformed FM clusters have uncorrelated moment orientations, and zero global magnetization. Note also that the "depth" of the QCP-like feature is not universal; it depends on the disorder strength.

To test the relevance of Fig. 3a to CMR manganites, a resistor network calculation was set up. Translating to Mn-oxide language, as explained previously, the MC generated configurations were mapped into a resistance grid (see caption of Fig. 3b). For up (down) spins, the blue regions of Fig. 2c—analog of positive magnetization FM clusters—have high (low) conductivity, the red regions have low (high) conductivity, and the green regions are insulating. The Kirchoff equations were solved exactly, leading to the results in Fig. 3b. In agreement with intuition, the nonpercolated state [Fig. 2c(2)] has a *large resistance* for both spins up and down, while the percolated low-T or disordered high-T states have far better conductance. Note that the resistance peak intensity increases as the ordering temperature is reduced by varying J_2, analog of $\langle r_A \rangle$, closer to the QCP-like regime.

The rotation of the large moments of the preformed FM clusters (Fig. 3a) may occur with small magnetic fields. These effects are mimicked in the toy model by using a staggered external field H_s which favors O_1 clusters with order parameter $M_s > 0$ (blue, Fig. 2c) to the detriment of O_1 clusters, with $-M_s$ (red, Fig. 2c), or O_2 regions. Figure 2d confirms the rapid generation of positive O_1 order in the region $T_{O_1} < T < T^*$ with tiny fields $0.01J_1$. This severely affects transport (Fig. 3c); i.e., a modest field transforms the intermediate T cluster state into a fairly uniform state with robust conductance. The results shown in Fig. 3c—the main results of this paper—are similar to those found in Mn oxides, and a huge MR ratio $[R(0) - R(H_s)]/R(H_s)$ of $\sim 4 \times 10^3\%$ was obtained at $H_s = 10^{-2}$ [17].

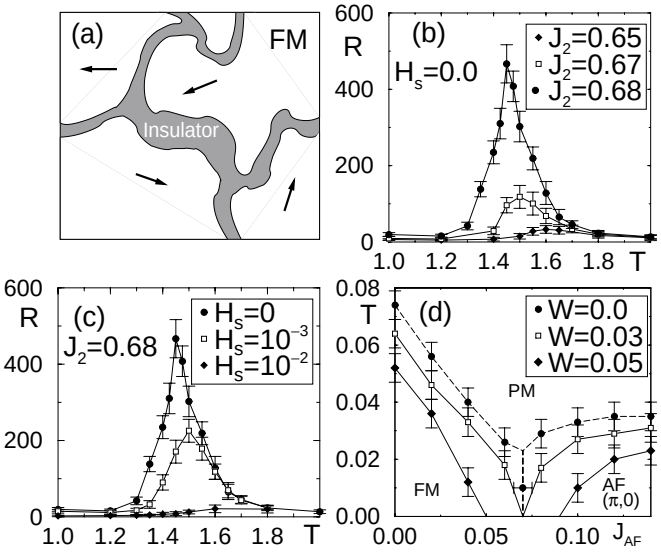

FIG. 3. (a) Proposed state for Mn oxides in the CMR regime. (b) Resistance of the toy model after the equivalence to manganite states is used (see text), using a 256^2 lattice, $W = 1.5$, at the couplings indicated. The calculation is carried out by transforming a spin configuration into a resistor network, with nodes centered at plaquettes (No. nodes $= 1/4$ No. sites) and with resistors between them. The values of the conductances of these resistors were established by using $BB = RR = 1.0$, $BR = 0$, $WW = 0.3$, $GG = BG = RG = WG = 0$, $WB = WR = 0.5$, where B, R, G, and W stand for blue, red, green, and white regions (see Fig. 2c), $AA' = \alpha$ means that the resistor between plaquettes in the A $(= B, R, G, W)$ and A' states has value α (arbitrary units), and $AA' = A'A$. Other values for WW and WB lead to similar results, and BB defines the scale. Note that the conductivity should be *spin dependent*, and a BR link (when an electron moves from a spin-up to a spin-down region) has zero conductance. The algorithm used to obtain the total conductance is exact [16]. (c) Resistance (arbitrary units) vs T, at external fields H_s indicated, using a 256^2 lattice, $J_2 = 0.68$, and $W = 1.5$. (d) T_C^* results for the one-orbital manganite model using 8^2 and 16^2 clusters, density $x = 0.5$, infinite Hund coupling, and hopping $t = 1$. With disorder, the J_{AF} couplings are randomly distributed between $J_{AF} - W$ and $J_{AF} + W$ (W indicated). In practice, T_C^* was defined when the spin correlations at distance $\sqrt{2}$ dropped below 40% of the maximum value.

In addition, there are already experimental indications in Mn oxides for the existence of a temperature scale T^* for uncorrelated cluster formation [18], which should be ubiquitous in low-bandwidth manganites [19].

The phase diagram in Fig. 1 is representative of more realistic models. Figure 3d contains MC results for the one-orbital model [20], in which the coupling J_{AF} between localized spins is varied to induce a metal-insulator transition [3]. Without disorder, the $T \sim 0$ transition is known to be first order between FM and AF states, the latter with rows or columns of spins up and down [3]. The "characteristic" ordering temperatures T_C^*, at which spin correlations become robust upon cooling, are shown vs J_{AF}. Note the similarity with Fig. 1.

The results in Figs. 1 and 2 can also be adapted to cuprates. The high-T_c phase diagram (inset of Fig. 1)

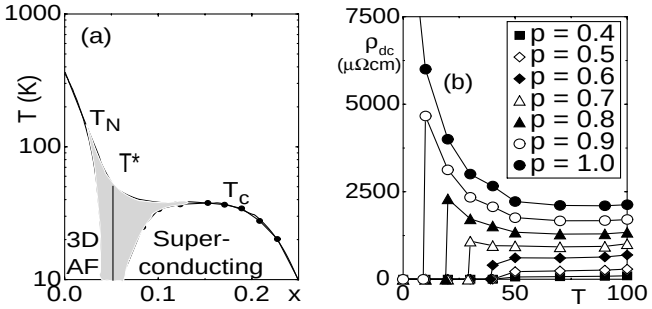

FIG. 4. (a) Conjectured HTS phase diagram. The black lines should be the actual phase boundaries without disorder. The shaded region is conjectured to have metallic (SC) and insulating (AF) coexisting regions in the real materials. (b) Resistivity ρ_{ab} vs T, from a random-resistor network calculation as in Ref. [24], where details can be found. A 50×50 cluster was used, with ρ_{ab} for insulating (optimal doping) fraction $p = 1.0$ (0.0) taken from LSCO $x = 0.04$ (0.15) data (see Ref. [26]). The inset labels are the p fractions at 100 K, all of which are smoothly reduced with decreasing T until percolation to a SC state occurs at $p = 0.5$.

shows a suppression of AF and SC order in a region usually labeled "spin glass," whose origin is unclear. Considering these diagrams together with the CPE results [10], it is conjectured that the very underdoped cuprate state may not be homogeneous but results from a SC vs *doped* AF competition after disorder is considered. Inhomogeneities (clusters) should be present even within ordered phases [Fig. 2c(3)]. Stripe states are candidates for the doped AF state [21].

The proposed clean-limit phase diagram is in Fig. 4a, with a vertical first-order transition line, which cuprates have upon electron doping [22], and heavy fermions with varying pressure. The shaded region may contain a mixture of stripelike and preformed SC islands [23]. Because of the general character of the discussion of Figs. 1 and 2, *colossal effects should be ubiquitous when ordered phases compete,* and they could appear in cuprates as well. CPE [10] could be a manifestation, with preformed SC clusters percolating under the influence of nearby SC materials. To further check this hypothesis, Fig. 4b contains results of a phenomenological random-resistor calculation of resistivity vs T [24], in rough agreement with experiments [25].

In summary, the results presented in this paper [27] suggest that colossal effects in TMO's could originate in intrinsic inhomogeneities. These large effects may be more general than previously anticipated. In our studies, the analog of the classical Griffiths regime—usually associated with weak effects—is here much more robust, strongly susceptible to external fields.

This work was supported by NSF-DMR-9814350 and the Computational Science and Information Technology school at Florida State University. The authors thank Y. Ando, D. N. Argyriou, S. L. Cooper, J. C. S. Davis, R. Decca, A. Feiguin, D. Gingold, N. Nagaosa, S. Sachdev, T. Senthil, P. Schiffer, and Y. Tokura for comments.

[1] Y. Tokura and N. Nagaosa, Science **288**, 462 (2000).
[2] J. Lynn *et al.,* Phys. Rev. Lett. **76**, 4046 (1996); J. De Teresa *et al.,* Nature (London) **386**, 256 (1997); J. Fernandez-Baca *et al.,* Phys. Rev. Lett. **80**, 4012 (1998); M. Uehara *et al.,* Nature (London) **399**, 560 (1999); M. Fäth *et al.,* Science **285**, 1540 (1999); I. Deac *et al.,* Phys. Rev. B **63**, 172408 (2001).
[3] E. Dagotto *et al.,* Phys. Rep. **344**, 1 (2001).
[4] Y. Tokura *et al.* (to be published).
[5] See *Quantum Phase Transitions,* edited by S. Sachdev (Cambridge University Press, Cambridge, UK, 1999).
[6] J. Hoshen *et al.,* Phys. Rev. B **14**, 3438 (1976).
[7] J. B. Torrance *et al.,* Phys. Rev. B **40**, 8872 (1989).
[8] S. H. Pan *et al.* (to be published); C. Howald *et al.,* cond-mat/0101251; K. M. Lang *et al.* (to be published).
[9] M.-H. Julien *et al.,* Phys. Rev. B **63**, 144508 (2001); A. W. Hunt *et al.,* cond-mat/0011380; Y. Sidis *et al.,* cond-mat/0101095; P. M. Singer *et al.,* cond-mat/0108291.
[10] R. S. Decca *et al.,* Phys. Rev. Lett. **85**, 3708 (2000).
[11] Y. Imry and S. Ma, Phys. Rev. Lett. **35**, 1399 (1975); E. Shimshoni *et al.,* Phys. Rev. Lett. **80**, 3352 (1998).
[12] R. B. Griffiths, Phys. Rev. Lett. **23**, 17 (1969).
[13] D. P. Landau, Phys. Rev. B **21**, 1285 (1980).
[14] M. Aizenman and J. Wehr, Phys. Rev. Lett. **62**, 2503 (1989); K. Hui and A. N. Berker, Phys. Rev. Lett. **62**, 2507 (1989). See also Y. Imry and M. Wortis, Phys. Rev. B **19**, 3580 (1979); J. Cardy, cond-mat/9806355.
[15] Quantum effects may be of relevance at low T [A. P. Young and H. Rieger, Phys. Rev. B **53**, 8486 (1996)].
[16] D. Frank and C. Lobb, Phys. Rev. B **37**, 302 (1988).
[17] By using a FM Ising model, P. Bastiaansen and H. Knops [J. Phys. Chem. Solids **59**, 297 (1998)] followed a procedure similar to ours to address CMR. The magnitude of the effect in this context is substantially smaller than in our calculations, where two phases are involved.
[18] Results compatible with a T^* well above T_C exist in manganites [De Teresa *et al.* (Ref. [2]); D. N. Argyriou *et al.,* Phys. Rev. B **60**, 6200 (1999)] and in EuO [C. S. Snow *et al.,* cond-mat/0011527].
[19] Mixed-phase regimes have a *pseudogap* in the density of states [A. Moreo *et al.,* Phys. Rev. Lett. **83**, 2773 (1999).
[20] J. L. Alonso *et al.,* Nucl. Phys. **B596**, 587 (2001).
[21] Frustrated phase separation without explicit quenched disorder could also further stabilize the effects described here [V. Emery and S. Kivelson, Physica (Amsterdam) **209C**, 597 (1993); J. Schmalian and P. Wolynes, Phys. Rev. Lett. **85**, 836 (2000)].
[22] N. Harima *et al.,* cond-mat/0103519.
[23] Preformed SC islands may have already been observed [I. Iguchi *et al.,* Nature (London) **412**, 420 (2001)].
[24] M. Mayr *et al.,* Phys. Rev. Lett. **86**, 135 (2001).
[25] N. Ichikawa *et al.,* Phys. Rev. Lett. **85**, 1738 (2000). See also M. Gutmann *et al.,* cond-mat/0009141; T. Egami, cond-mat/0102449. Figure 4a is related to SO(5) ideas [S. C. Zhang, Science **275**, 1089 (1997)].
[26] H. Takagi *et al.,* Phys. Rev. Lett. **69**, 2975 (1992); see also Y. Ando *et al.,* cond-mat/0104163.
[27] Details will be provided elsewhere.